Controlling the potential landscape and normal modes of ion Coulomb crystals by a standing-wave optical potential

Thomas Lauprêtre,[1] Rasmus B. Linnet,[1] Ian D. Leroux,[1,2] Haggai Landa,[3] Aurélien Dantan,[1] and Michael Drewsen[1,*]

[1]*Department of Physics and Astronomy, Aarhus University, DK-8000 Aarhus C, Denmark*
[2]*National Research Council Canada, Ottawa, Ontario, Canada K1A 0R6*
[3]*Institut de Physique Théorique, Université Paris-Saclay, CEA, CNRS, F-91191 Gif-sur-Yvette, France*

Light-induced control of ions within small Coulomb crystals is investigated. By intense intracavity optical standing-wave fields, subwavelength localization of individual ions is achieved for one-, two-, and three-dimensional crystals. Based on these findings, we illustrate numerically how the application of such optical potentials can be used to tailor the normal-mode spectra and patterns of multidimensional Coulomb crystals. The results represent, among others, important steps towards controlling the crystalline structure of Coulomb crystals, investigating heat-transfer processes at the quantum limit, and quantum simulations of many-body systems.

Introduction. Trapped ions, laser cooled into long-range-ordered structures, so-called Coulomb crystals, are a prime example of strongly correlated matter systems which are of broad relevance for plasma, solid-state, and atomic physics [1,2], as well as astrophysics, and whose unique properties make it possible to experimentally investigate various fundamental classical and quantum many-body systems [3–12]. They also represent well-controlled systems for cavity quantum electrodynamics [13–17], quantum simulation [3–5,18], and cold chemistry experiments [19,20].

The additional application of optical potentials to trapped ions enlarges the range of possible applications. For instance, the interplay between optical and Coulomb forces can be used to investigate friction at the nanoscale [12,21–29], the dynamics of ions in quantum potentials [30,31], or energy transport in coupled oscillator systems [23,32–35]. Optical forces on ions can potentially also be exploited for pure optical trapping [36–38], useful for the investigation of ultracold interactions between ions and neutrals [37,39–42].

So far, experimental investigations of ion dynamics in optical lattices have been limited to single ions [43–46] or small one-dimensional crystals [17,25,27,28,47] in radio-frequency traps. In this Rapid Communication, we investigate the control of the potential landscape and normal modes of Coulomb-interacting particles in multidimensional Coulomb crystals by a standing-wave optical potential. Depending on the relative strengths of the Coulomb and optical forces, various regimes of interest may be considered: (i) When the optical potential is stronger than the Coulomb and trapping potentials, the ions can be pinned along the standing-wave field direction. We investigate this regime experimentally by demonstrating simultaneous subwavelength localization of up to eight ^{40}Ca$^+$ ions in one-, two- and three-dimensional Coulomb crystals. In addition to the above-mentioned applications, the results

are promising, e.g., for inhibiting spontaneous, thermally activated crystalline structure changes observed in large Coulomb crystals [48], as optical lattice potentials such as those applied here have been theoretically predicted to stabilize and enable the deterministic control of their crystalline structure [49]. (ii) When the optically induced forces are comparable to those of the trapping potential, the application of the optical potential can be used to tailor, in a static or dynamic fashion, the normal modes of the crystals. We investigate this regime numerically and show the occurrence of nontrivial normal-mode dynamics for the experimentally realized multidimensional structures. Such a tailoring opens a different playground for fundamental investigations of energy-transfer processes at the atomic scale, in which dimensionality plays a role [33,34]. It could also have important applications in connection with quantum many-body simulations with ion crystals in Penning traps [50–52] or Paul traps [53–56], for which using standing-wave optical potentials for tailoring the normal modes of two-dimensional crystals [52,57,58] would be a complementary alternative to the application of traveling waves [7,11] and potentially enlarge the toolbox for engineering effective spin-spin interactions.

Experimental setup. In the experiments, a number of ^{40}Ca$^+$ ions is produced and confined in a linear Paul trap as described in detail in Refs. [59,60] (Fig. 1). The trap operates at a radio frequency (rf) of $\sim$3.98 MHz, with axial and radial trap frequencies in the range 70–110 and 180–400 kHz, respectively. The ions are first Doppler cooled for 62 μs, then optically pumped for 75 μs to the $|D_{3/2}, m = +3/2\rangle$ state ($>$98% efficiency per ion on average) by the combined application of light fields close to resonance with the $S_{1/2} \rightarrow P_{1/2}$ (397 nm) and $D_{3/2} \rightarrow P_{1/2}$ (866 nm) transitions in the presence of a 2.2-G bias magnetic field along the z axis (see Ref. [13]). The resulting Coulomb crystal has a typical interion distance of the order of $\sim$20 μm. An 11.8-mm-long linear Fabry-Pérot cavity with moderate finesse ($\sim$3000) and waist radius $\sim$37 μm allows for the generation of a standing wave along the z axis with intensity up to $\sim$500 kW/cm^2 at the center of the
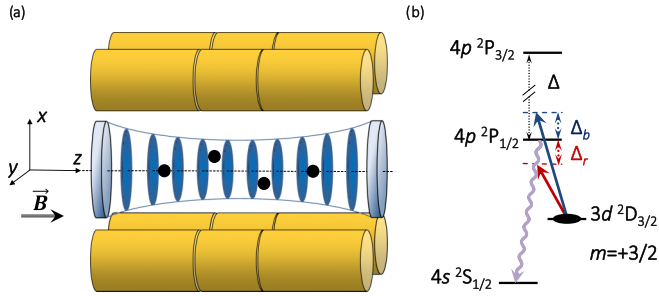
*drewsen@phys.au.dk

FIG. 1. (a) Experimental setup: Ions trapped in a linear Paul trap and arranged in a Coulomb crystal are pinned along the z direction by an intracavity standing-wave field. (b) Relevant energy levels in ^{40}Ca$^+$. The long blue and short red straight arrows represent excitations by blue- or red-detuned standing-wave fields. The purple wavy arrow represents the subsequent emitted and detected photon. $\Delta/(2\pi) \sim 6.7$ THz is the frequency difference between the $P_{1/2}$ and $P_{3/2}$ states.

trap. Ions are positioned at the absolute center of the optical cavity following the method of Ref. [61]. After switching off the optical pumping fields, a σ^- circularly polarized standing-wave field detuned either to the blue or the red side of the $D_{3/2} \rightarrow P_{1/2}$ transition by ± 0.76 THz is ramped up for 2 μs [45] and held at its maximum level for 1 μs. An independent and absolute calibration of the lattice potential depth experienced by a single ion as a function of the intensity transmitted out of the cavity is used as a reference [62], and a maximum lattice depth $T_{\text{latt}} \sim 25$ mK, corresponding to a lattice vibrational frequency $\nu_{\text{latt}} \sim 3.7$ MHz [63], can be reached at this detuning in the limit of available laser power. When an ion is excited to the $P_{1/2}$ state by the intracavity field, it leaves the $|D_{3/2}, m = +3/2\rangle$ state with 97% probability by subsequently decaying to either the $|D_{3/2}, m = \pm 1/2\rangle$ states (3%) or predominantly to the $S_{1/2}$ state (94%) where it no longer interacts with the standing wave [64]. The 397-nm photons scattered in the latter case are detected by an intensified CCD camera, gated to be active only during the 3 μs when the standing wave is applied.

Experimental results. The measured scattering probability per ion and per experimental sequence is plotted in Fig. 2 as a function of the optical lattice depth for three different spatial configurations of the ions, a one-dimensional eight-ion string, a two-dimensional four-ion zigzag crystal, and a three-dimensional six-ion octahedron crystal [65], obtained for axial and radial trap frequencies of (70, 350), (85, 170), and (105, 190) kHz, respectively. The insets in Fig. 2 show fluorescence images of these crystals. To break the symmetry of the radial trapping potentials and improve the long-term orientational stability of the zigzag and octahedron crystals, a small bias voltage resulting in a $\sim$3% difference in the radial frequencies was applied. In the experiments, the orientational or configurational changes of the crystals occurred at a rate of $\sim$2 and $\sim$4 s^{-1} for the zigzag and octahedron crystals, respectively. As detailed in the Supplemental Material [66], the initial average axial temperature of the ions in each configuration is evaluated by measuring their position variance based on the detected fluorescence images prior to the application of the optical lattice, and calculating numerically the frequency
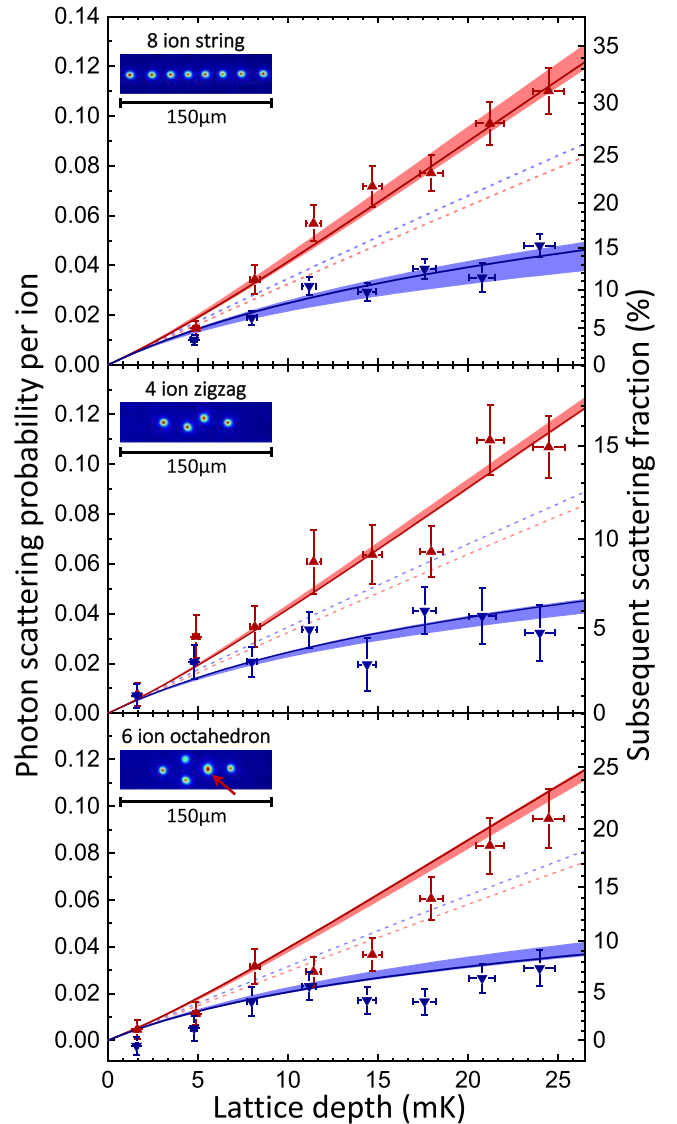

FIG. 2. Photon scattering probability per ion and per sequence as a function of the optical lattice depth for an eight-ion string (top), a two-dimensional four-ion zigzag crystal (center), and a three-dimensional six-ion octahedron crystal (bottom). The red up triangles/blue down triangles are experimental data points for the red–plx-sol-plxblue-detuned lattices. Each data point corresponds to the repetition of approximately 2×10^6 sequences. The upper red and lower blue shaded areas are the theoretical scattering probabilities computed from the measured initial temperatures, with the thickness representing their error bar. The upper red and lower blue continuous lines are the best results from single free-parameter fits to the data. The upper red and lower blue dashed lines show the theoretical scattering probabilities expected for delocalized ions; the slight asymmetry between scattering probabilities from red- and blue-detuned lattices is due to the non-negligible excitation to the $P_{3/2}$ state which is taken into account in the model. The red arrowhead on the fluorescence picture at the bottom indicates two out-of-plane ions overlapping.

of the normal modes of motion from the axial and radial frequencies of the trap [67,68]. For the three crystals shown in Fig. 2, the axial temperatures are found to be 3.6 ± 1.1, 3.5 ± 0.5, and 3.1 ± 0.5 mK, respectively.

Analysis and discussion. Under these conditions, the initial position distribution of each ion extends over several lattice periods, so that the variation of the background trapping potential over one lattice period is small with respect to the initial thermal energy. Moreover, given the relatively large interion distances used in this work, the lattice-induced forces quickly overcome the trapping and Coulomb forces along the axis as the lattice intensity is ramped up over a timescale comparable to or shorter than the inverse of the secular axial frequencies. As such, the ions can be expected to independently localize close to the minima (maxima) of intensity of the blue- (red-) detuned standing-wave field, as demonstrated with a single ion in Ref. [45]. In principle, the scattering dynamics of a multi-ion crystal are more complex than for a single ion, since, as soon as one ion gets excited by the standing-wave field, it will decay with almost unit probability to a state which is not affected by the lattice (see above). However, in the limit where the probability of exciting more than one ion in each sequence is low, the detected scattering is essentially that of the first excited ion, thus providing information on its average position distribution inside the lattice potential before any depinning event. We therefore base the analysis on the single-ion model of Ref. [45], which, given the initial temperature of the ions, yields a prediction of the probability per ion to have scattered a photon during the application of the standing wave by determining the position distribution in the lattice at each instant [66].

The predictions of the model based on the independently measured initial temperatures are shown in Fig. 2 (shaded areas) for each configuration [69], and are generally observed to be in very good agreement with the experimental data points. For the octahedron crystal, one observes, though, a general tendency of the data points to lie below the theoretical curves. This fact is likely due to a globally reduced measured scattering probability as a result of more frequent configurational changes (4 s^{-1}) and heating of the entire structure followed by slow recrystallization ($\gg$ms) occurring over the long acquisition period of 5 min per data point. As an alternative analysis, we also show in Fig. 2 the best-fit results of the theoretical model [Eqs. (1) and (2) in Ref. [66]] to the data points with the initial temperature only left as a single free parameter (solid lines). Such fits yield initial temperatures of 4.0 ± 0.5, 3.9 ± 0.9, and 2.7 ± 0.8 mK, respectively, in very good agreement with the temperatures independently determined from the fluorescence images. The resulting uncertainties on the scattering probability (not shown) are similar to the ones obtained via the first analysis based on the initial temperature measurements. Note that this analysis does not include reduced scattering due to heating of the crystal either.

In addition, we show on the right scale of the graphs of Fig. 2 the subsequent scattering fraction, i.e., the fraction of the signal that is due to the detection of any other photon than the first emitted one [66]. The single-ion model is observed to give accurate predictions not only for all blue-detuned lattice data points, for which this fraction is always less than 15%, but also for the red-detuned lattice data points, for which this fraction may be substantially higher. This may seem surprising since, as soon as one ion in a crystal scatters a photon from the standing-wave field excitation, it decays with almost unit probability to a state which is not affected by

the lattice and therefore changes the total potential energy of the system. The change in potential energy of the ions still affected by the optical lattice could possibly lead to a change in the localization process as their configuration changes, which would then alter subsequent scattering events. The experiment should, however, be insensitive to such effects for two reasons. First, the interaction time with the lattice (3 μs in total) is never much longer than the period of the highest-frequency normal mode (2.6 μs in the lowest case of the eight-ion string). Consequently, the system has too little time to relax and redistribute thermal energy between ions after a scattering event. Second, since the initial position distribution of each ion extends over several lattice sites, crystal distortions due to pinning or depinning alter the potential energy of the system by only a fraction of the initial thermal energy.

Using the model predictions based on the experimentally determined initial temperatures [66], we infer the "bunching parameter" $B = \langle \sin^2(kz) \rangle$, which represents the averaged normalized potential distribution (B is 0 for ions perfectly localized at the potential minima and $1/2$ for completely delocalized ions). For each of the configurations of Fig. 2 pinned inside the deepest blue-detuned lattice field ($\sim$25 mK) the inferred values are 0.22 ± 0.03, 0.22 ± 0.01, and 0.22 ± 0.02, respectively, which clearly indicate that subwavelength localization in the optical potential is achieved.

Micromotion. A general concern when experimenting with ion Coulomb crystals in linear rf traps is the rf-induced micromotion. Even for experiments with a single ion, where the ion in principle can be trapped on an rf nodal line, the ion's dynamics can be compromised due to resonances between the rf drive and the ion's oscillation in the optical potential [36,44,45]. For multidimensional crystals, some ions will furthermore always be positioned away from the rf-field-free nodal line with a resulting micromotion radial kinetic energy which can easily exceed the thermal energy of the ion by orders of magnitude [70,71]. For instance, the off-axis ions of the zigzag and octahedron crystals of Fig. 2 are estimated to have micromotion radial kinetic energies corresponding to $\sim$160 and $\sim$800 mK, respectively. Due to the general coupling between the axial and radial motional degrees of freedom, it is hence not immediately clear that the axial optical pinning of ions in such crystals can be achieved by realistic experimental optical potential depths of only $\sim$25 mK. A theoretical analysis confirmed by numerical simulations at 0 K shows, however, that the micromotion kinetic energy due to the Coulomb interaction along the rf-field-free direction is typically several orders of magnitude smaller than the radial micromotion kinetic energies in a linear Paul trap, both with and without the optical potential present [71,72]. For instance, for the four-ion zigzag crystal, the amplitude of the axial micromotion of the external ions in a 25-mK-deep lattice is $\sim$4 $\times$ 10^{-3} times lower than the off-axis ion radial micromotion amplitude, corresponding to 0.35% of the lattice period and an additional axial kinetic energy of $\sim$3 μK. Residual micromotion due to potential parasitic axial components of the rf field could be more of a concern. An experimentally determined upper bound of its amplitude in the absence of lattice for the eight-ion string leads to a maximal associated kinetic energy less than 0.4 mK for the outer ions. According to the numerical simulations, this could lead, in
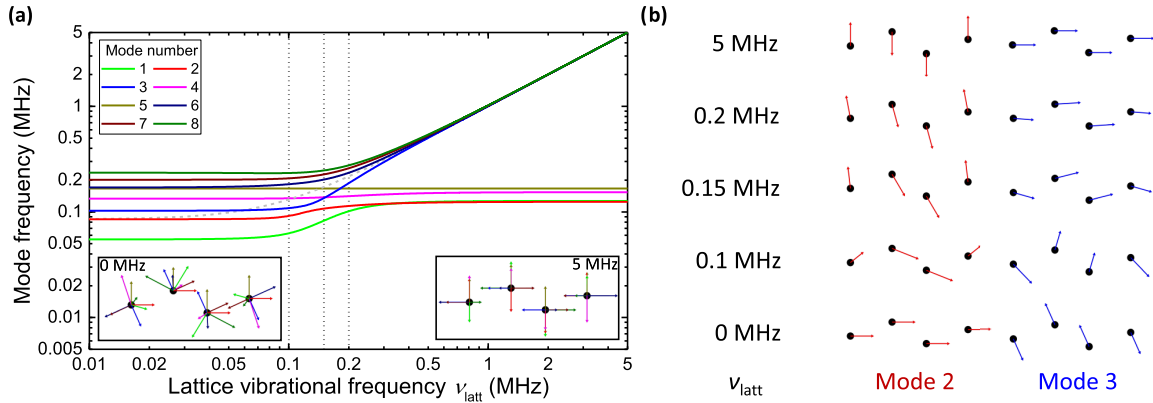
FIG. 3. (a) Evolution of the frequency of the in-plane normal modes of the four-ion zigzag configuration as a function of the lattice vibrational frequency ν_{latt}. As a reference, the center-of-mass mode frequency of a single ion is shown by the gray dashed line. The two insets show the mode coordinates (in relative units) without a lattice (0 MHz) and in the presence of the deepest lattice (5 MHz). (b) Evolution of the coordinates of modes 2 and 3 [whose frequencies in the absence of lattice are respectively the second and third lowest, and shown by the red and blue lines in (a)], for low and high lattice frequencies (0 and 5 MHz) and around the avoided crossing [0.1, 0.15, and 0.2 MHz, indicated by the vertical dotted lines in (a)].

the presence of a 25-mK-deep lattice potential, to an axial micromotion amplitude of up to ~17% of the lattice period (corresponding kinetic energy ~8 mK) for these ions. Such an excess micromotion would, though, only contribute to the observed values of $\langle \sin^2(kz) \rangle$ by a few percent.

Normal-mode spectrum. We finally turn to the prospect of tailoring the normal-mode spectrum and patterns of Coulomb crystals by the application of an optical lattice potential. To this end, we have numerically calculated the parametric continuation of the normal modes as a function of the lattice depth for the three crystals presented in this Rapid Communication. Results obtained for the four-ion zigzag configuration are shown in Fig. 3(a), and for the other crystals in Ref. [66]. As observed, the mode spectrum changes dramatically when changing the lattice from being a weak perturbation to becoming the dominant axial confining potential. At the latter point, the axial and radial motional degrees of freedom nearly completely decouple, and all axial modes have identical frequencies. This degeneracy of the purely axial modes could, e.g., facilitate the simultaneous resolved sideband laser cooling [73] or cavity cooling [74] of all axial modes to the ground state by applying just a single-frequency laser. While the radial mode frequencies do not become degenerate for strong axial confinement, they cluster though within a significantly narrower distribution than without a lattice. Consequently, this scenario might facilitate the ground-state electromagnetically induced transparency (EIT) cooling [75] of all radial modes with fixed laser frequencies. Combining the two strategies for axial and radial cooling should be an interesting route to initialize small ion systems near their quantum mechanical ground state, which would be of relevance for investigating energy transport and thermodynamics in the quantum regime.

A perhaps even more remarkable feature is the complex evolution of the individual modes at moderate lattice depths. As an example, Fig. 3(b) illustrates how the center-of-mass mode (mode 2) and an essentially radial mode (mode 3) in the absence of a lattice are switching their nature as the lattice

depth is adiabatically increased. One can envision several applications of this feature. For instance, both these modes could potentially be cooled to the ground state by combining direct sideband cooling of only one of the two modes at a lattice depth outside the switching ("avoided crossing") area with fast nonadiabatically ramping of the lattice through the avoided crossing and adiabatically back again. Furthermore, by clever combinations of adiabatic and nonadiabatic rampings of the lattice potential, one might eventually be able to cool a larger number of modes.

From a many-body physics perspective, the avoided crossings could be exploited to engineer Hamiltonians with specific effective mode couplings [50,51,53–56], and one could, e.g., investigate the decoherence of superpositions of excitations of several of the modes converging to axial modes with the same frequencies at the deep lattices after applying various ramping sequences. Since the highly nontrivial normal-mode dynamics strongly depends on the dimensionality as well as the number of ions, as illustrated in Ref. [66], the combination of ion Coulomb crystals with an optical potential opens an exciting playground for investigating, exploiting, and engineering complex interactions between phonon modes.

Conclusion. We have experimentally demonstrated the subwavelength localization of ions in multidimensional ion Coulomb crystals by applying intense optical standing-wave fields. The fact that micromotion in these multidimensional ion crystal structures does not impede the lattice-induced localization is very promising not only for achieving deterministic control of the crystalline structure of cold charged plasmas [49], but also for tailoring the complex dynamics of their normal modes with applications within the energy transport at the quantum limit as well as quantum many-body physics. As the specific coupling achievable between modes depends on the dimensionality and number of ions, it expands the possibilities for tuning complex interactions in these strongly coupled systems, and may eventually be used in simulations of "artificial" molecules.

[1] D. H. E. Dubin and T. M. O'Neil, Rev. Mod. Phys. **71**, 87 (1999).

[2] M. Drewsen, J. Phys. B **460**, 105 (2015).

[3] D. Porras and J. I. Cirac, Phys. Rev. Lett. **92**, 207901 (2004).

[4] R. Blatt and C. Roos, Nat. Phys. **8**, 277 (2012).

[5] C. Schneider, D. Porras, and T. Schaetz, Rep. Prog. Phys. **75**, 024401 (2012).

[6] A. Bermudez, T. Schaetz, and D. Porras, New J. Phys. **14**, 053049 (2012).

[7] J. W. Britton, B. C. Sawyer, A. C. Keith, C.-C. J. Wang, J. K. Freericks, H. Uys, M. J. Biercuk, and J. J. Bollinger, Nature (London) **484**, 489 (2012).

[8] K. Chen, S. T. Sullivan, W. G. Rellergert, and E. R. Hudson, Phys. Rev. Lett. **110**, 173003 (2013).

[9] S. Genway, W. Li, C. Ates, B. P. Lanyon, and I. Lesanovsky, Phys. Rev. Lett. **112**, 023603 (2014).

[10] S. J. Schowalter, A. J. Dunning, K. Chen, P. Puri, C. Schneider, and E. R. Hudson, Nat. Commun. **7**, 12448 (2016).

[11] J. G. Bohnet, B. C. Sawyer, J. W. Britton, M. L. Wall, A. M. Rey, M. Foss-Feig, and J. J. Bollinger, Science **352**, 1297 (2016).

[12] J. Kiethe, R. Nigmatullin, D. Kalincev, T. Schmirander, and T. E. Mehlstäubler, Nat. Commun. **8**, 15364 (2017).

[13] P. F. Herskind, A. Dantan, J. P. Marler, M. Albert, and M. Drewsen, Nat. Phys. **5**, 494 (2009).

[14] M. Albert, A. Dantan, and M. Drewsen, Nat. Photonics **5**, 633 (2011).

[15] B. Casabone, A. Stute, K. Friebe, B. Brandstätter, K. Schüppert, R. Blatt, and T. E. Northup, Phys. Rev. Lett. **111**, 100505 (2013).

[16] B. Casabone, K. Friebe, B. Brandstätter, K. Schüppert, R. Blatt, and T. E. Northup, Phys. Rev. Lett. **114**, 023602 (2015).

[17] S. Begley, M. Vogt, G. K. Gulati, H. Takahashi, and M. Keller, Phys. Rev. Lett. **116**, 223001 (2016).

[18] C. Hempel, C. Maier, J. Romero, J. McClean, T. Monz, H. Shen, P. Jurcevic, B. P. Lanyon, P. Love, R. Babbush *et al.*, Phys. Rev. X **8**, 031022 (2018).

[19] S. Willitsch, M. T. Bell, A. D. Gingell, and T. P. Softley, Phys. Chem. Chem. Phys. **10**, 7200 (2008).

[20] S. Willitsch, *Proceedings of the International School of Physics "Enrico Fermi"*, Vol. 189 (IOS, Amsterdam, 2015), p. 255.

[21] I. Garcia-Mata, O. Zhirov, and D. Shepelyansky, Eur. Phys. J. D **41**, 325 (2007).

[22] A. Benassi, A. Vanossi, and E. Tosatti, Nat. Commun. **2**, 236 (2011).

[23] T. Pruttivarasin, M. Ramm, I. Talukdar, A. Kreuter, and H. Häffner, New J. Phys. **13**, 075012 (2011).

[24] M. Cetina, A. Bylinskii, L. Karpa, D. Gangloff, K. M. Beck, Y. Ge, M. Scholz, A. T. Grier, I. Chuang, and V. Vuletić, New J. Phys. **15**, 053001 (2013).

[25] A. Bylinskii, D. Gangloff, and V. Vuletić, Science **348**, 1115 (2015).

[26] T. Fogarty, C. Cormick, H. Landa, V. M. Stojanović, E. Demler, and G. Morigi, Phys. Rev. Lett. **115**, 233602 (2015).

[27] D. Gangloff, A. Bylinskii, I. Counts, W. Jhe, and V. Vuletić, Nat. Phys. **11**, 915 (2015).

[28] A. Bylinskii, D. Gangloff, I. Counts, and V. Vuletić, Nat. Mater. **15**, 717 (2016).

[29] J. Kiethe, R. Nigmatullin, T. Schmirander, D. Kalincev, and T. E. Mehlstäubler, New J. Phys. **20**, 123017 (2018).

[30] P. Bushev, A. Wilson, J. Eschner, C. Raab, F. Schmidt-Kaler, C. Becher, and R. Blatt, Phys. Rev. Lett. **92**, 223602 (2004).

[31] C. Cormick and G. Morigi, Phys. Rev. Lett. **109**, 053003 (2012).

[32] M. Ramm, T. Pruttivarasin, and H. Häffner, New J. Phys. **16**, 063062 (2014).

[33] A. Ruiz, D. Alonso, M. B. Plenio, and A. del Campo, Phys. Rev. B **89**, 214305 (2014).

[34] N. Freitas, E. A. Martinez, and J. P. Paz, Phys. Scr. **91**, 013007 (2016).

[35] A. Abdelrahman, O. Khosravani, M. Gessner, H.-P. Breuer, A. Buchleitner, D. J. Gorman, R. Masuda, T. Pruttivarasin, M. Ramm, P. Schindler *et al.*, Nat. Commun. **8**, 15712 (2017).

[36] C. Schneider, M. Enderlein, T. Huber, and T. Schätz, Nat. Photonics **4**, 772 (2010).

[37] T. Huber, A. Lambrecht, J. Schmidt, L. Karpa, and T. Schaetz, Nat. Commun. **5**, 5587 (2014).

[38] J. Schmidt, A. Lambrecht, P. Weckesser, M. Debatin, L. Karpa, and T. Schaetz, Phys. Rev. X **8**, 021028 (2018).

[39] A. T. Grier, M. Cetina, F. Oručević, and V. Vuletić, Phys. Rev. Lett. **102**, 223201 (2009).

[40] C. Zipkes, S. Palzer, L. Ratschbacher, C. Sias, and M. Köhl, Phys. Rev. Lett. **105**, 133201 (2010).

[41] S. Schmid, A. Härter, and J. H. Denschlag, Phys. Rev. Lett. **105**, 133202 (2010).

[42] M. Cetina, A. T. Grier, and V. Vuletić, Phys. Rev. Lett. **109**, 253201 (2012).

[43] H. Katori, S. Schlipf, and H. Walther, Phys. Rev. Lett. **79**, 2221 (1997).

[44] M. Enderlein, T. Huber, C. Schneider, and T. Schaetz, Phys. Rev. Lett. **109**, 233004 (2012).

[45] R. B. Linnet, I. D. Leroux, M. Marciante, A. Dantan, and M. Drewsen, Phys. Rev. Lett. **109**, 233005 (2012).

[46] C. T. Schmiegelow, H. Kaufmann, T. Ruster, J. Schulz, V. Kaushal, M. Hettrich, F. Schmidt-Kaler, and U. G. Poschinger, Phys. Rev. Lett. **116**, 033002 (2016).

[47] L. Karpa, A. Bylinskii, D. Gangloff, M. Cetina, and V. Vuletić, Phys. Rev. Lett. **111**, 163002 (2013).

[48] M. Drewsen, T. Matthey, A. Mortensen, and J. Petter Hansen, arXiv:1202.2544.

[49] P. Horak, A. Dantan, and M. Drewsen, Phys. Rev. A **86**, 043435 (2012).

[50] C.-C. J. Wang, A. C. Keith, and J. K. Freericks, Phys. Rev. A **87**, 013422 (2013).

[51] P. Richerme, Phys. Rev. A **94**, 032320 (2016).

[52] G. Stutter, P. Hrmo, V. Jarlaud, M. K. Joshi, J. F. Goodwin, and R. C. Thompson, J. Mod. Opt. **65**, 549 (2018).

[53] R. Nath, M. Dalmonte, A. W. Glaetzle, P. Zoller, F. Schmidt-Kaler, and R. Gerritsma, New J. Phys. **17**, 065018 (2015).

[54] B. Yoshimura, M. Stork, D. Dadic, W. C. Campbell, and J. K. Freericks, EPJ Quantum Technol. **2**, 2 (2015).

[55] S. Ding, G. Maslennikov, R. Hablützel, H. Loh, and D. Matsukevich, Phys. Rev. Lett. **119**, 150404 (2017).

[56] G. Maslennikov, S. Ding, R. Hablutzel, J. Gan, A. Roulet, S. Nimmrichter, J. Dai, V. Scarani, and D. Matsukevich, Nat. Commun. **10**, 202 (2019).

[57] T. B. Mitchell, J. J. Bollinger, D. H. E. Dubin, X.-P. Huang, W. M. Itano, and R. H. Baughman, Science **282**, 1290 (1998).

[58] S. Mavadia, J. F. Goodwin, G. Stutter, S. Bharadia, D. R. Crick, D. M. Segal, and R. C. Thompson, Nat. Commun. **4**, 2571 (2013).

[59] P. Herskind, A. Dantan, M. B. Langkilde-Lauesen, A. Mortensen, J. L. Sørensen, and M. Drewsen, Appl. Phys. B **93**, 373 (2008).

[60] P. F. Herskind, A. Dantan, M. Albert, J. P. Marler, and M. Drewsen, J. Phys. B **42**, 154008 (2009).

[61] R. B. Linnet, I. D. Leroux, A. Dantan, and M. Drewsen, Appl. Phys. B **114**, 295 (2014).

[62] T. Laupretre, O. Legrand, P. Neveu, A. Dantan, and M. Drewsen (unpublished).

[63] The lattice frequency is defined as $\nu_{\text{latt}} = \frac{k}{2\pi}\sqrt{\frac{2k_{\text{B}}T_{\text{latt}}}{M}}$, where k is the standing-wave field wave number, k_{B} the Boltzman constant, and M the mass of the ion.

[64] The probability of interacting again with the lattice field, and subsequently heating the ion, after a decay to the $|D_{3/2}, m = +1/2\rangle$ state (2%) is very low, due to the smaller Clebsch-Gordan coefficient and dipole element.

[65] The octahedron crystal has a structure that has an S_4 symmetry, i.e., it maps back onto itself by a combination of a 90° rotation around the axis connecting the two ions furthest apart and a reflection across the central plane perpendicular to this axis.

[66] See Supplemental Material at http://link.aps.org/supplemental/10.1103/PhysRevA.99.031401 for additional experimental and simulation results, as well as details on the theoretical models used for data analysis.

[67] S. Knünz, M. Herrmann, V. Batteiger, G. Saathoff, T. W. Hänsch, and T. Udem, Phys. Rev. A **85**, 023427 (2012).

[68] V. Rajagopal, J. P. Marler, M. G. Kokish, and B. C. Odom, Eur. J. Mass Spectrom. **22**, 1 (2016).

[69] For the zigzag and the octahedron crystals, the lower light intensity experienced by the off-axis ions has also been accounted for.

[70] D. Berkeland, J. Miller, J. Bergquist, W. Itano, and D. Wineland, J. Appl. Phys. **83**, 5025 (1998).

[71] H. Landa, M. Drewsen, B. Reznik, and A. Retzker, New J. Phys. **14**, 093023 (2012).

[72] H. Landa, M. Drewsen, B. Reznik, and A. Retzker, J. Phys. A **45**, 455305 (2012).

[73] D. J. Wineland, R. E. Drullinger, and F. L. Walls, Phys. Rev. Lett. **40**, 1639 (1978).

[74] T. Fogarty, H. Landa, C. Cormick, and G. Morigi, Phys. Rev. A **94**, 023844 (2016).

[75] G. Morigi, J. Eschner, and C. H. Keitel, Phys. Rev. Lett. **85**, 4458 (2000).